Robotica (2011) volume 29, pp. 1049–1057. © Cambridge University Press 2011
doi:10.1017/S0263574711000300

Biologically inspired motion synthesis method of two-legged robot with compliant feet*

Teresa Zielinska† and Andrzej Chmielniak

Warsaw University of Technology, Institute of Aeronautics and Applied Mechanics (WUT–IAAM), ul. Nowowiejska 24, 00-665 Warsaw, Poland

(Received in Final Form: March 10, 2011. First published online: April 13, 2011)

SUMMARY

This work presents biologically inspired method of gait generation. It uses the reference to the periodic signals generated by biological central pattern generator. The coupled oscillators with correction functions are used to produce leg joint trajectories. The human gait is the reference pattern. The features of generated gait are compared to the human walk. The spring-loaded foot design is presented together with experimental results.

KEYWORDS: Biomimetic robots; Bipeds; Control of robotic systems; Design; Legged robots.

1. Introduction

The majority of body functions, such as beating of the heart, breathing, chewing, and locomotion, is periodic.[4] In human, walking-synchronized displacement of all main parts of the body is noticeable. Longitudinal and lateral rotation of the trunk, pelvis, and twist of shoulders is coordinated with the states of walking cadence (moment of foot touching the ground, foot lift-off, middle stance, etc.).[12,17] The single inverted pendulum or spring loaded inverted pendulum is often used as the simplified mechanical model of human gait.

In recent years, there are many attempts to get the two-legged robots moving as the human.[3,11] However, to obtain the robot movement similar to human is still a problem due to the mechanical construction limits or due to the weaknesses of motion generation methods.[10] The biologically inspired methods of gait generation refers to the neural generators of living rhythms (in that is also the walking rhythm). A broad discussion of advantages of utilizing central pattern generators (CGPs) in robotics can be found in ref. [7], and an interesting overview of the different oscillators utilized for robotics purposes is given in ref. [4]. By contrast to the pendulum-based methods, where the mechanical parameters of construction predetermine the synthesized motion pattern, the oscillators-based methods focuses on sensory feedbacks (gait synthesis using Matsuoka oscillators[9]) or on close imitation of biological gait features (leg transfers sequences or joint angles). Therefore, the mechanical structure must be able to follow the motion pattern.

The research being conducted at the Warsaw University of Technology aims at developing biologically inspired motion patterns[18] for legged robots. We consider the coupled oscillators – the type of oscillators for which the closed-form solution does not exist. Those oscillators couplings synchronize not only the joint positions, but also their higher order derivatives. The analysis of those oscillators is difficult. The analytical form does not include the information from the sensors.

The biped robot consisting of the lower extremities and the torso is meant to serve as a research platform for presented method of motion synthesis. Robot has 12 active degrees of freedoms (DOFs). The design structure is illustrated in Fig. 1. To reduce the masses, the elements were cut by laser in aluminum rectangular segments.

2. Robot Gait

2.1. Motion pattern

Our method refers to the biological CPGs and to the conclusion of Bernstein[2] concerning the scheme of human motion skills development. According to ref. [2] in learning the motion abilities, three stages exist. In the first stage (early infancy), the reduction of DOF is visible – by random displacements, the baby learns how to produce the highly coupled simple rhythmic movements. The second stage includes freeing the previously locked DOFs and producing complex motions on the basis of first governed rhythms. The third stage enhances motion efficiency by using the advantages of passive dynamics, inertial effects, etc. Referring to this concept in our work, we first produce the periodic motion trajectories for leg joints. For the search of parameters describing the trajectories, a genetic algorithm is used. The role of the penalty functions used here can be compared to the qualitative learning experience gained by the baby. As the equivalent of biological CPGs, we use equations of coupled oscillators for compact "storing" of the fundamental rhythmic pattern. Fine tuning of the shape of the trajectories is obtained by the correction functions. This is the stage of adding complexity to the previously learned rhythmic, but not obviously fully correct, motion pattern. The third stage where human uses the advantages of passive dynamics and other dynamic effects was realized in our work

* This paper was originally submitted under the auspices of the CLAWAR Association. It is an extension of work presented at CLAWAR 2009: the 12th International Conference on Climbing and Walking Robots and the Support Technologies for Mobile Machines, Istanbul, Turkey.

† Corresponding author. E-mail: teresaz@meil.pw.edu.pl

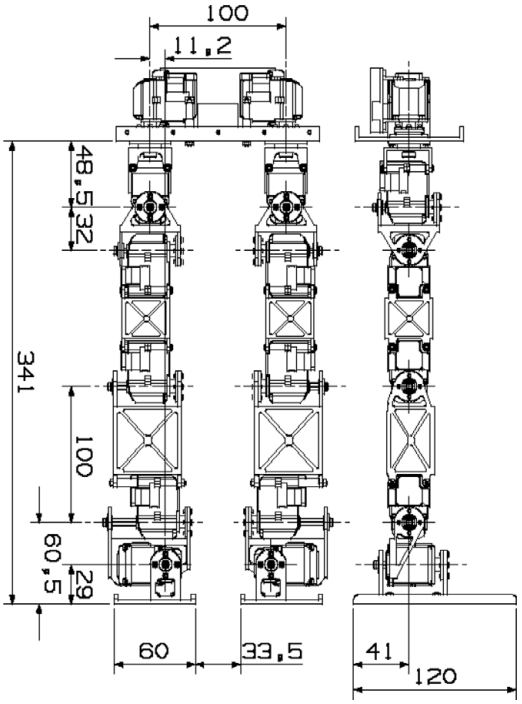

Fig. 1. Front and side view of the assembly with dimensions analyzed in one of the calculations (the torso is not included).

by heuristic addition of pelvis rotation. The advantage of applying the coupled oscillators for modeling of the CPGs rhythm is the compactness of the trajectories description and possibility of fast tuning of parameters in analytical equations for following the arbitrarily chosen rhythmic trajectories. The equations describing the dynamical properties of oscillators have the following general form:

$$\ddot{x}_{osc} - \mu \cdot \left(p^2 - x_{osc}^2\right) \cdot \dot{x}_{osc} + g^2 \cdot x_{osc} = q. \qquad (1)$$

The variables μ, p^2, g^2, q influence the properties of oscillators. Cyclic solutions of coupled oscillators formula are interpreted as the legs joint trajectories.[1] Specifically, the changes of angle in the hip and knee joints for both legs are described by the following four oscillators:

$$\begin{aligned}
\ddot{\alpha}_1 - \mu_1 \cdot \left(p_1^2 - x_a^2\right) \cdot \dot{\alpha}_1 + g_1^2 \cdot x_a &= q_1,\\
\ddot{\alpha}_2 - \mu_2 \cdot \left(p_2^2 - x_b^2\right) \cdot \dot{\alpha}_2 + g_2^2 \cdot x_b &= q_2,\\
\ddot{\alpha}_3 - \mu_3 \cdot \left(p_3^2 - x_c^2\right) \cdot \dot{\alpha}_3 + g_3^2 \cdot x_c &= q_3,\\
\ddot{\alpha}_4 - \mu_4 \cdot \left(p_4^2 - x_d^2\right) \cdot \dot{\alpha}_4 + g_4^2 \cdot x_d &= q_4,
\end{aligned} \qquad (2)$$

where

$$\begin{aligned}
x_a &= \alpha_1 - \lambda_{21} \cdot \alpha_2 - \lambda_{31} \cdot \alpha_3,\\
x_b &= \alpha_2 - \lambda_{12} \cdot \alpha_1 - \lambda_{42} \cdot \alpha_4,\\
x_c &= \alpha_3 - \lambda_{13} \cdot \alpha_1 - \lambda_{43} \cdot \alpha_4,\\
x_d &= \alpha_4 - \lambda_{24} \cdot \alpha_2 - \lambda_{34} \cdot \alpha_3.
\end{aligned}$$

These equations have 24 parameters: μ_1, μ_2, μ_3, μ_4, p_1^2, p_2^2, p_3^2, p_4^2, g_1^2, g_2^2, g_3^2, g_4^2, q_1, q_2, q_3, q_4,

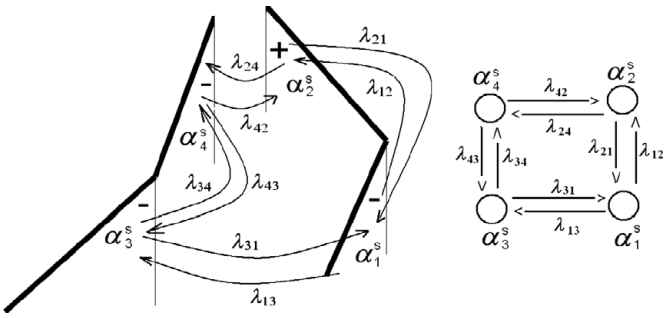

Fig. 2. Definition of angles and illustration of joint couplings.

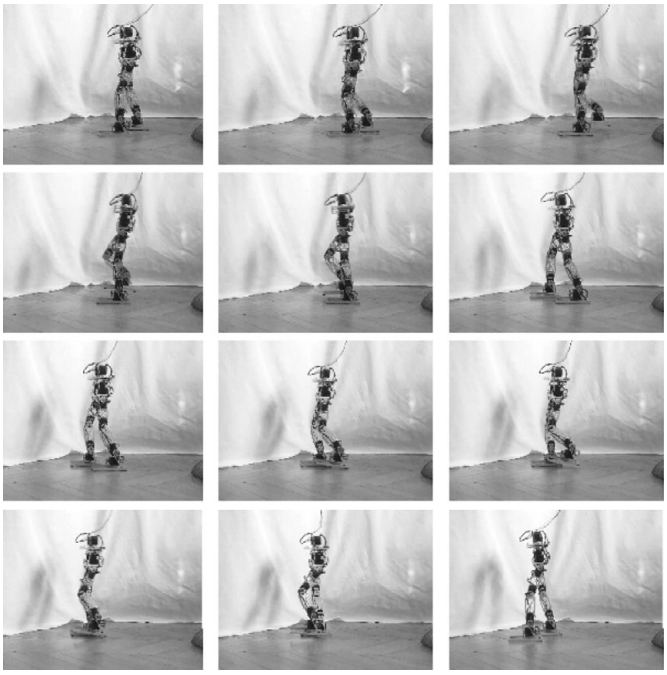

Fig. 3. Robot in walk.

λ_{13}, λ_{31}, λ_{12}, λ_{21}, λ_{24}, λ_{42}, λ_{43}, λ_{34}. The coupling parameters λ_{ij} mainly determine the type of gait – they influence the phase shift between the trajectories. The influence of the coupling parameters as well as the other parameters to the trajectories of α_i is not possible to specify in coupled oscillators formula. The results of some study on it were presented in ref. [18]. The angles α_1^s, α_2^s, α_3^s, α_4^s correspond to the adequately scaled α_1, α_2, α_3, α_4. It is assumed that the angles α_i^s are positive, if the thigh or shank is in front of the vertical line and negative if it is begin (Fig. 2, Fig. 3). The coupling terms λ_{ij} through x_a to x_d define the influence of α_1^s to α_j^s. Figure 2 illustrates the notation. The variables α_i and α_i^s represent the values expressed in degrees.

The trajectories recorded during human walk were considered as the reference. The motion was sampled every 0.021 s. The recorded data were processed and evaluated using the specialized software combined with the VICON motion recording system. It was confirmed that the person (healthy young man) walks with statistically verified, representative gait (Fig. 4). The gait period was 1.04 s, walking speed was 1.53 m/s, the support phase was about 60% of the gait period, in this the double support phase took 10% of the gait period. Those values match

https://doi.org/10.1017/S0263574711000300 Published online by Cambridge University Press

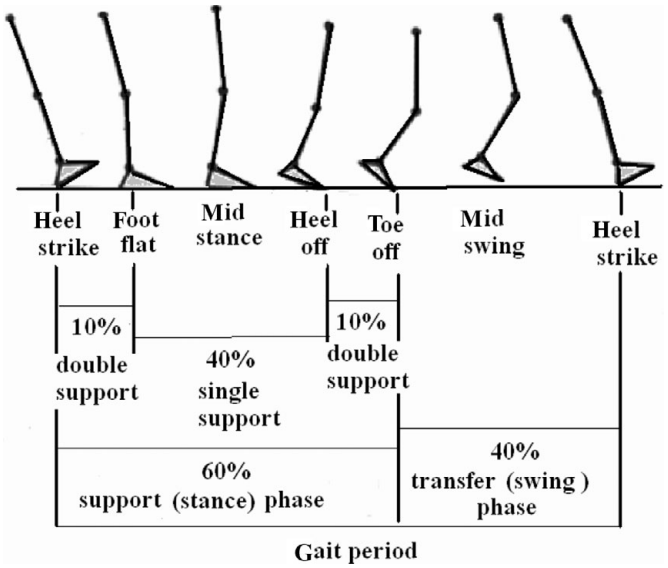

Fig. 4. Phases of human gait.

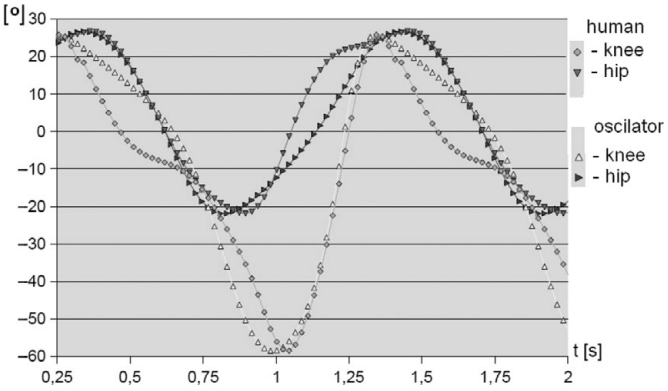

Fig. 5. Joint trajectories for human gait and the generated gait (for one leg).

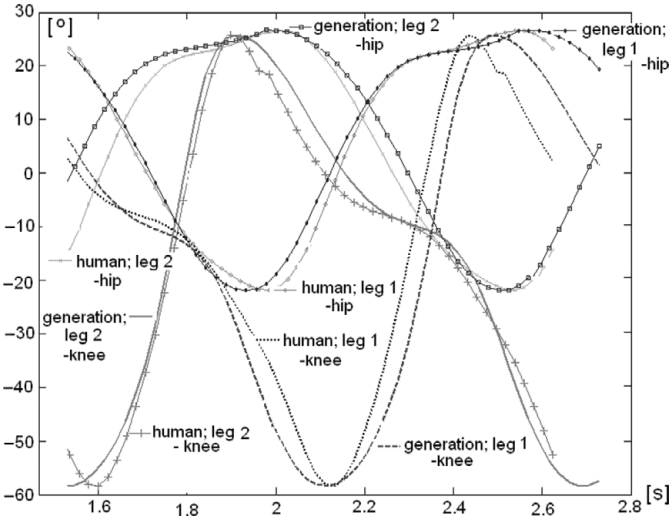

Fig. 6. Obtained joint trajectories compared to the human gait.

the norm established for human gait.[12,17] To imitate more closely the biological learning process and to get the accuracy in reproducing the gait rhythm, a genetic algorithm for oscillators parameters evaluation was applied.

The search started from the previously identified set of parameters:[18] $\mu_1 = 1,\ \mu_2 = 2,\ \mu_3 = 1,\ \mu_4 = 2,$

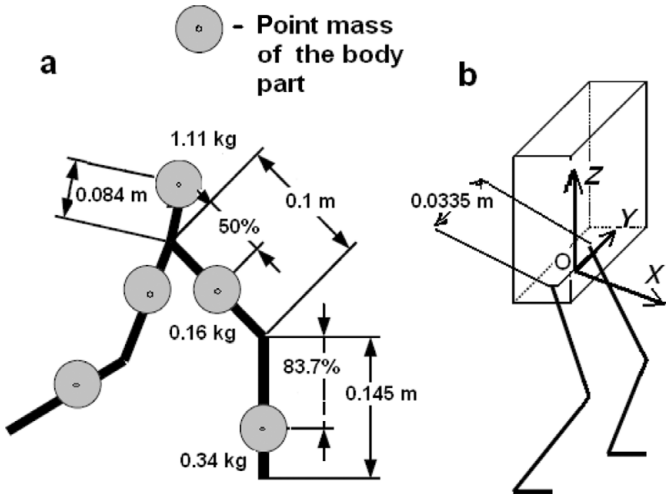

Fig. 7. Simplified model of the robot.

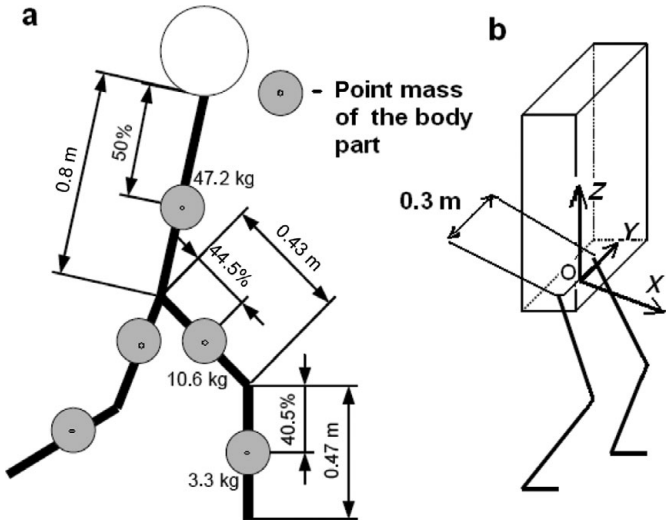

Fig. 8. Simplified model of human body.

$p_1^2 = 1,\ p_2^2 = 1, p_3^2 = 1,\ p_4^2 = 1, g_1^2 = 17,\ g_2^2 = 20, g_3^2 = 17,\ g_4^2 = 20,\ q_1 = 12,\ q_2 = -20,\ q_3 = 12,\ q_4 = -20,\ \lambda_{13} = 0.2,\ \lambda_{31} = 0.2,\ \lambda_{12} = -0.2,\ \lambda_{21} = -0.2,\ \lambda_{24} = 0.2, \lambda_{42} = 0.2,\ \lambda_{43} = -0.2, \lambda_{34} = -0.2.$

The details on genetic-algorithm-based parameters tuning are given in ref. [19]; therefore, we will give here only the summary of it. The fitness function consisted of the sum of square errors between generated and measured leg joint angles:

$$f_j = \frac{\sum_{i=1}^{n} \left(\alpha_j^h(i) - \alpha_j^s(i)\right)^2}{n}, \tag{3}$$

where $\alpha_j^h(i)$ is the value of jth joint angle in human walk obtained in the ith data instant, $\alpha_j^s(i)$ is the angle obtained from the generator, and n is the number of data registered for one walking step. The six penalties with experimentally chosen ranges (over those ranges oscillators were unstable) were introduced. The penalties were as following: s_1 – penalty weight considering interlimb coordination, this penalty was maximal ($s_1 = 5$) when both legs were moving together, s_2 – penalty weight for unstable oscillations

https://doi.org/10.1017/S0263574711000300 Published online by Cambridge University Press

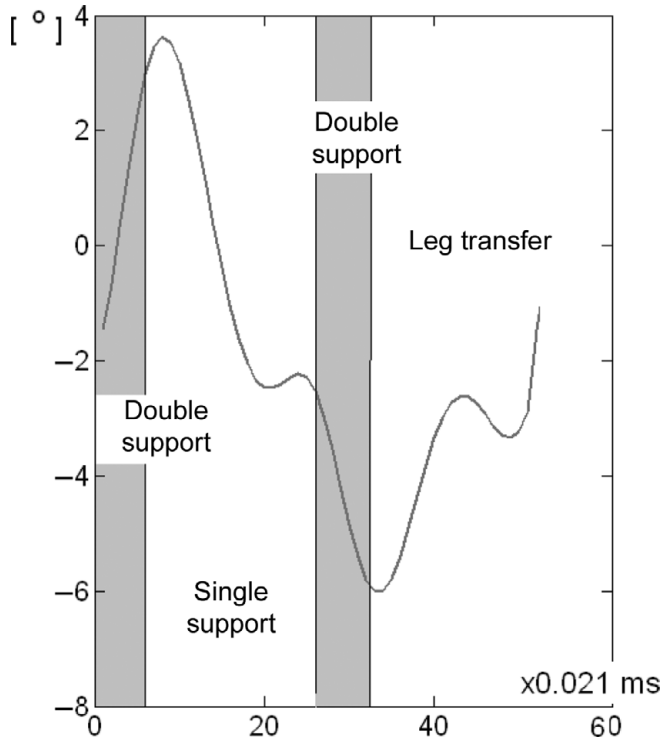

Fig. 9. Human's pelvis rotation (up and down in frontal plane).

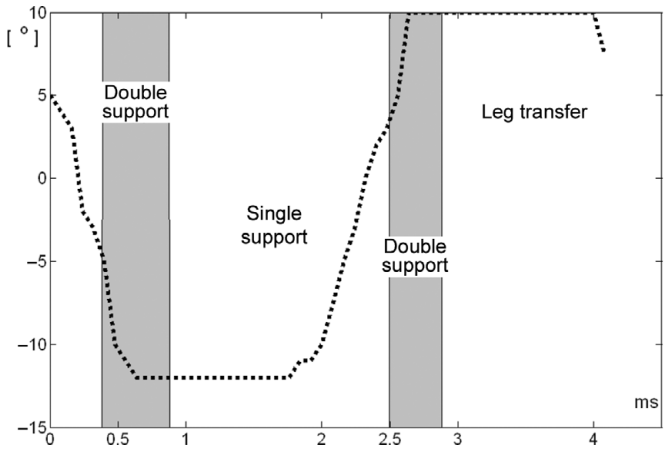

Fig. 10. Robot's pelvis rotation (up and down in frontal plane).

(maximal $s_2 = 10$), s_3 – penalty weight for backward movement of torso (maximal $s_3 = 3$), s_4 – penalty weight for backward movement of the foot (maximal $s_4 = 3$), s_5 – penalty weight for lack of foot forward motion (maximal $s_5 = 3$), s_6 – penalty weight for abnormal knee bend (maximal $s_6 = 3$). If any of the listed above conditions was not fulfilled the appropriate penalty assumed its minimum – $s_i = 1$. The overall fitness function was

$$FF_G = -(f_1 + f_2 + f_3 + f_4) \cdot \prod_{k=1,\ldots,6} s_k. \qquad (4)$$

Figure 5 illustrates the obtained joint trajectories compared to the human gait. The oscillators parameters are as follows: $\mu_1 = \mu_3 = 3.59375$, $\mu_2 = \mu_4 = 2$, $p_1^2 = p_3^2 = 2$, $p_2^2 = p_4^2 = 1, g_1^2 = g_3^2 = 28.0039, g_2^2 = g_4^2 = 17.7031, q_1 = q_3 =$

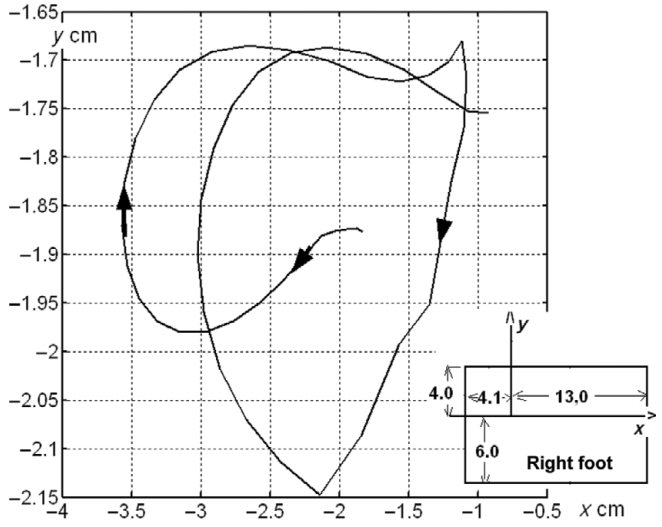

Fig. 11. ZMP trajectory for human gait evaluated using human body model with consideration of trunk inclination (double support phase is included, the foot frame is shown).

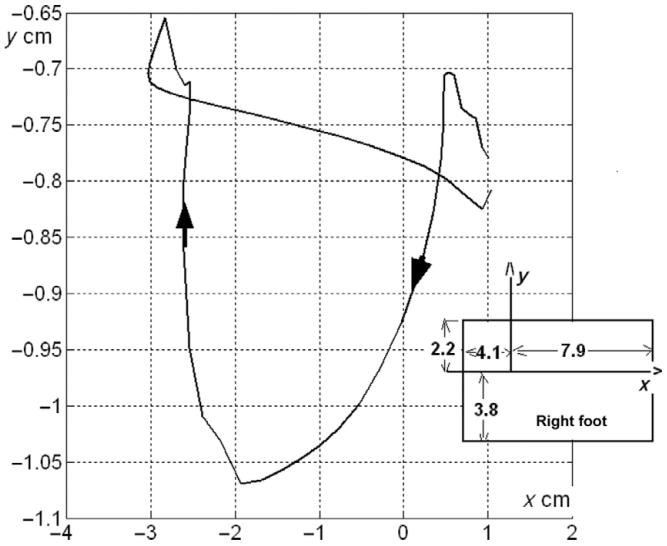

Fig. 12. ZMP trajectory for modified robot gait with trunk inclination (double support phase is included, the foot frame is shown).

15.8516, $q_2 = q_4 = -7.04492$, $\lambda_{12} = \lambda_{21} = \lambda_{34} = \lambda_{43} = -0.451172, \lambda_{24} = \lambda_{42} = \lambda_{31} = \lambda_{13} = 0.417969$. In the next stage of motion learning (according to N. A. Bernstein), movement complexity is increased to obtain motions reaching targets, such as rhythmic walk and walk with gait transitions. Following this, the next aim was to mimic closely the human gait. The addition (or subtraction) of smooth function increasing from zero to some maximum and next decreasing, with its derivative being equal to zero at the ends of the definition range can produced appropriate correction of joint trajectories. We chose

$$F_{corr} = A\ cos^2(\phi) \quad \phi = \langle -\Pi/2, \Pi/2 \rangle, \qquad (5)$$

amplitude A can be positive or negative depends on for which joint (hip or knee) it is used. With added corrections, the generated and real gait trajectories almost overlap (see Fig. 6).

https://doi.org/10.1017/S0263574711000300 Published online by Cambridge University Press

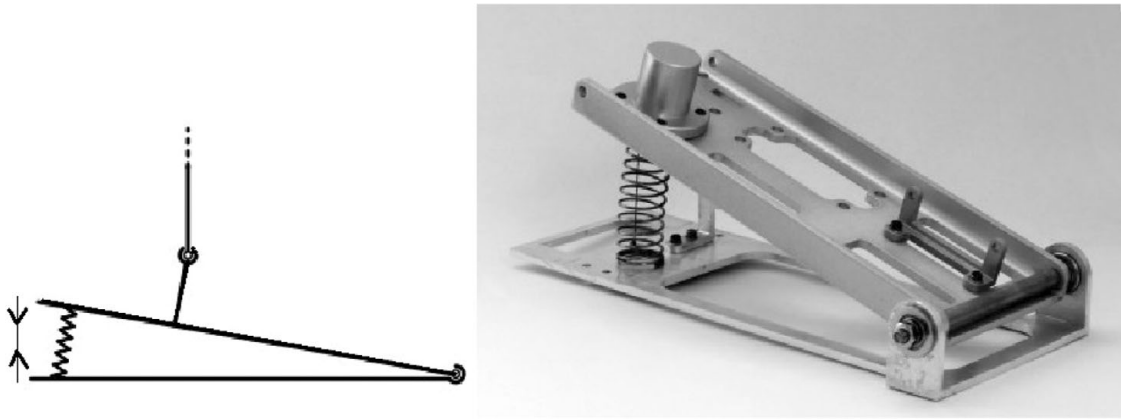

Fig. 13. New foot.

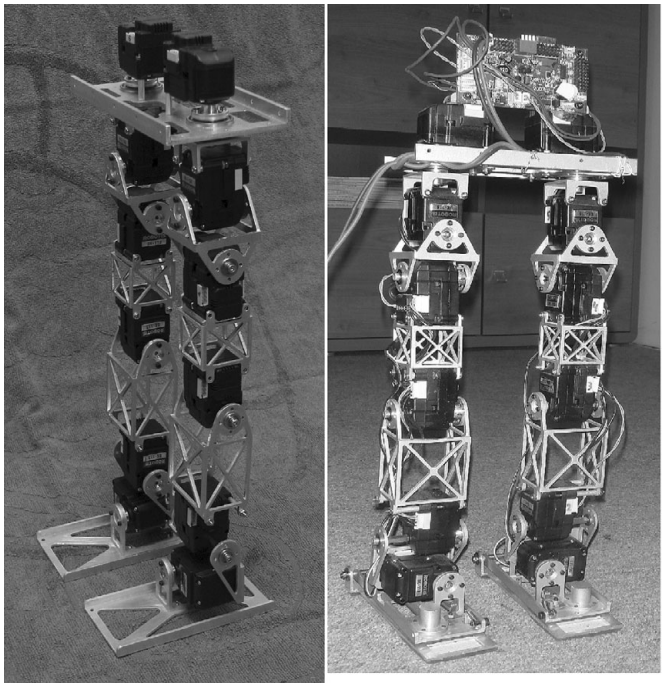

Fig. 14. Robot with simple feet - left, robot with new compliant feet - right.

2.2. Motion implementation

Final synthesis of the robot motion requires us to take into account the selected indicators (ZMP, pelvis movement properties) describing the human gait. The time courses of those indicators were obtained for the kinematic models with point masses for the human and the robot bodies. The differences between those indicators were due to differences in human and robot structure – especially lack of upper body part in robot. We adjusted the robot motion to obtain the considered indicators close to the human and the point mass model of the human body was considered. Masses of body parts and link dimensions were assumed from anthropomorphic data for the person whose gait was recorded. The body build was typical for the 95% centile level. Motion was synthesized for a legged robot with only the legs and upper part of the body being a cube (3D structure, the upper part of the human body was also simplified to a point mass assuming that the upper limbs remain motionless during walking. With this simplification, the model of human body consisted of five parts – two shanks together with feet, two thighs, and one part representing the whole upper part.

Robot prototype was 0.3295 m tall, with length of thigh equal to 0.10 m and shank with foot equal to 0.145 m. The mass of the robot was 1.61 kg, with thigh mass equal to

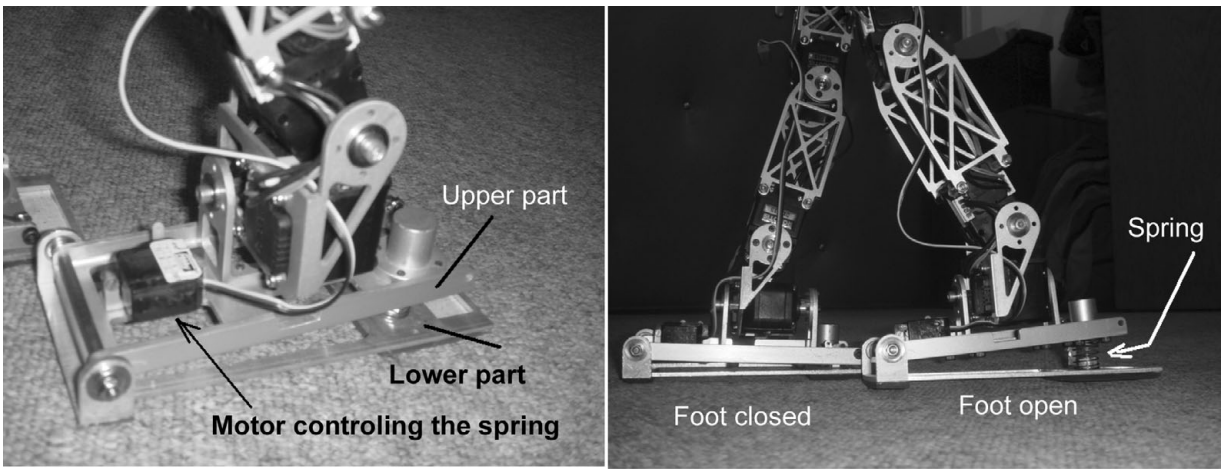

Fig. 15. Pictures of robot's new feet: right picture – left foot is in open (spring released position) during leg takeoff, right foot is closed in full support phase.

https://doi.org/10.1017/S0263574711000300 Published online by Cambridge University Press

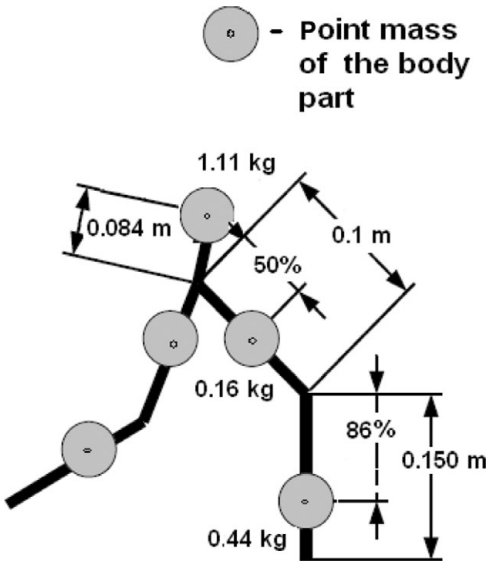

Fig. 16. Mass distribution of the robot with modified feet.

0.16 kg, shank with foot equal to 0.34 kg, and in that foot equal to 0.10 kg. The distance between the ground projection of the robot ankle and rear of the foot was 0.041 m. The point mass of thigh was located below the hip joint at a distance equal to half of thigh length. Point mass of the shank considered together with foot was located below the knee at a distance equal to 83.7% of the shank segment length. Legs were about 3.7 times shorter than in the human. The structures of robot and human bodies are presented in Figs. 7 and 8. The dynamical modeling (ZMP calculation) was performed using our own software with Newton–Euler formulation in 3D space. The details regarding ZMP can be found in many publications (see, e.g., refs. [15] and [16]). The following formula produces the coordinates x_{ZMP}, y_{ZMP} of the point F_{ZMP}:

$$x_{ZMP} = \frac{\sum_i^n m_i(\ddot{z}_i - g)x_i - \sum_i^n m_i\ \ddot{x}_i\ z_i - \sum_i^n I_i^y \ddot{\alpha}_i^y}{\sum_i^n m_i(\ddot{z}_i - g)}, \quad (6)$$

$$y_{ZMP} = \frac{\sum_i^n m_i(\ddot{z}_i - g)y_i - \sum_i^n m_i\ \ddot{y}_i\ z_i - \sum_i^n I_i^x \ddot{\alpha}_i^x}{\sum_i^n m_i(\ddot{z}_i - g)}, \quad (7)$$

where m_i is the mass of the ith body part, x_i, y_i, z_i are the coordinates of mass center of the ith part expressed in the frame attached to the trunk, $\ddot{x}_i$, $\ddot{y}_i$ $\ddot{z}_i$ are accelerations of those points with respect to this frame, I_i^x, I_i^y are the main moments of inertia for ith body part about X- and Y-axes, $\ddot{\alpha}_i^x$, $\ddot{\alpha}_i^y$ are the angular accelerations about those axes, and g is the gravity constant.

Applying the human motion pattern to robot ZMP calculation, it was detected that at the end of the robot single support phase the ZMP was outside the back of the footprint – the posture was not equilibrated. This was also confirmed in reality. First walking experiments were not successful. The robot was falling back, what was expected considering the position of the ZMP. Moreover, it was found that not all servo motors produce the same speed and the control step must be again increased to 0.08 what resulted in gait period equal to 4 s. Concerning ZMP, the gait was modified. The ranges of hip joint trajectories were shifted toward positive direction reducing the leg-end backward shift at the end of the support phase and increasing the forward shift at the beginning of the support phase. In the knee, a small bend during the support phase was added. Using the reference to human motion, the robot rolling (trunk inclination in the frontal plane) was introduced. That referred to the feature of human gait, however it did not exactly imitate it (see Figs. 9 and 10). The resultant time course of the ZMP was similar to that observed in human walk (compare Figs. 11 and 12).

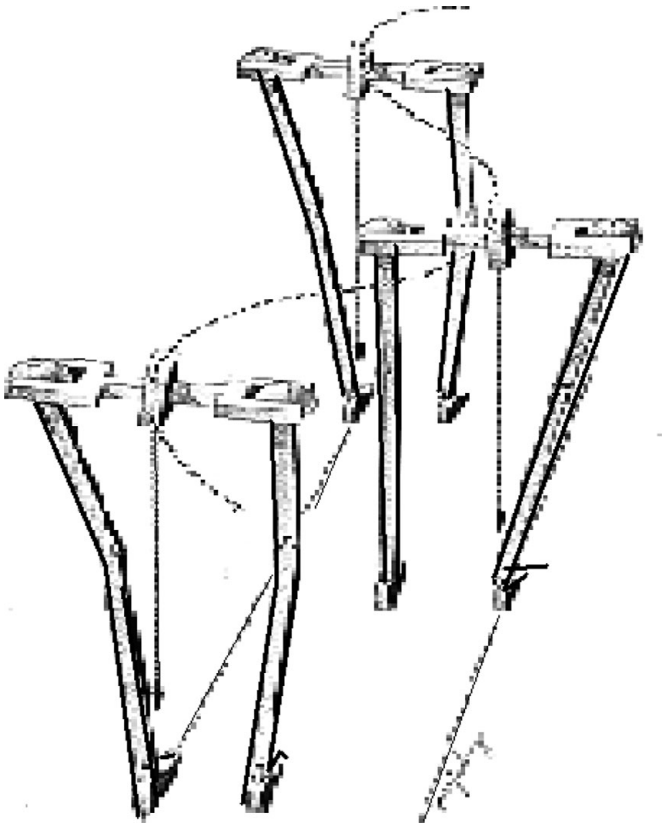

Fig. 17. Lateral pelvic displacement in human walk.

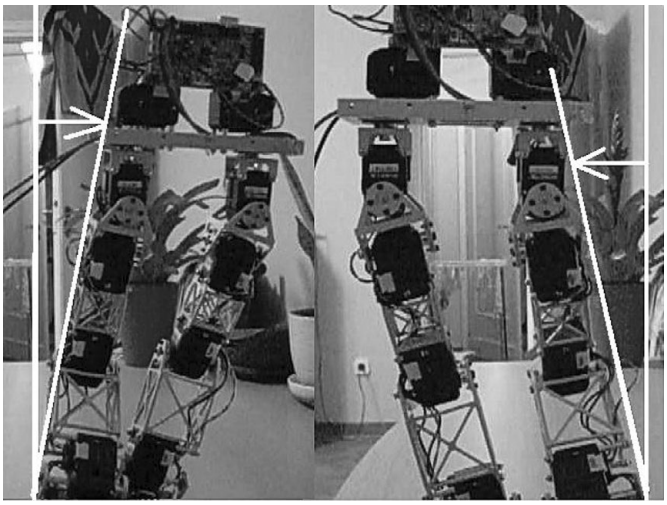

Fig. 18. Lateral displacement of robot upper body.

https://doi.org/10.1017/S0263574711000300 Published online by Cambridge University Press

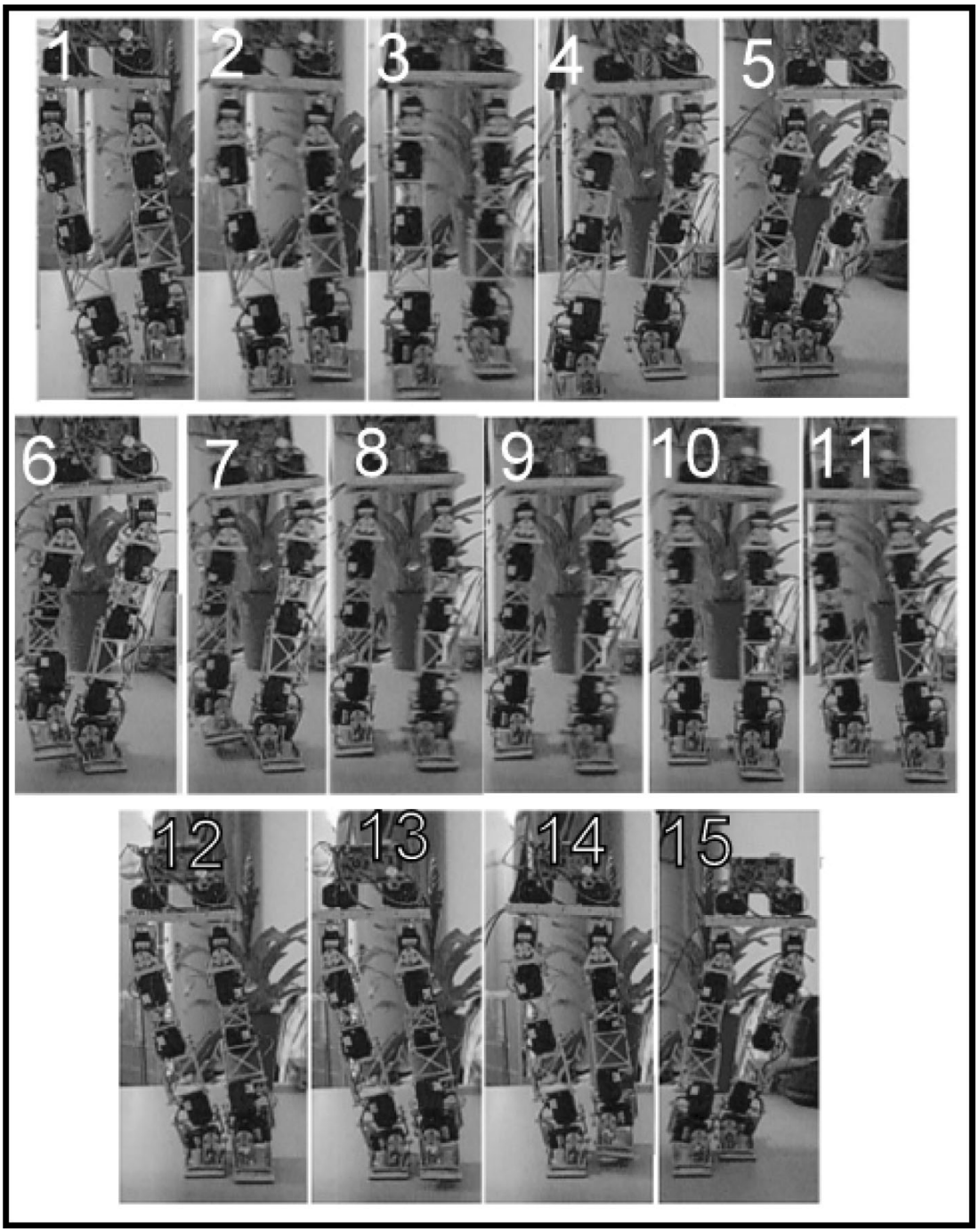

Fig. 19. Robot in walk: sequence from left to right, first – upper line.

3. Spring-Loaded Foot

The elaborated gait pattern was implemented in the biped, details and results are discussed in ref. [19]. After successful implementation of gait, the robot's feet were replaced by the modified one, with in-build springs (see Figs. 13 and 14). The new foot consists of two, instead of one main element as previously, spring is located in the heel (Fig. 15). This increases the weight. The motor controlling the spring release is also located in the foot. Foot modification besides of changing the robot upper leg mass distribution (compare Figs. 7 and 16) affected robot motion performances. The mounting of two moving parts introduced small horizontal backlash, the spring locking mechanism has also latch backlash along vertical direction appearing in locking position. Because of that it was needed the adjustment of previously implemented gait. In first stage, it was done keeping the spring in locked – compressed position (closed foot). The lack of upper body increasing the motion stability made the gait tuning task difficult. The stability during leg transfer required significant pelvic displacements. In some extend, it is similar to human motion performance where the pelvis traces a sinusoidal curve with an amplitude of approximately 0.06 m.[13] The pick of this transfer occurs at the end of mid stance (see Fig. 17). As is illustrated in Fig. 18 in single support phase, the robot is inclined to side for about 10^0, the pelvis central point side shift is about 0.04 m. This

https://doi.org/10.1017/S0263574711000300 Published online by Cambridge University Press

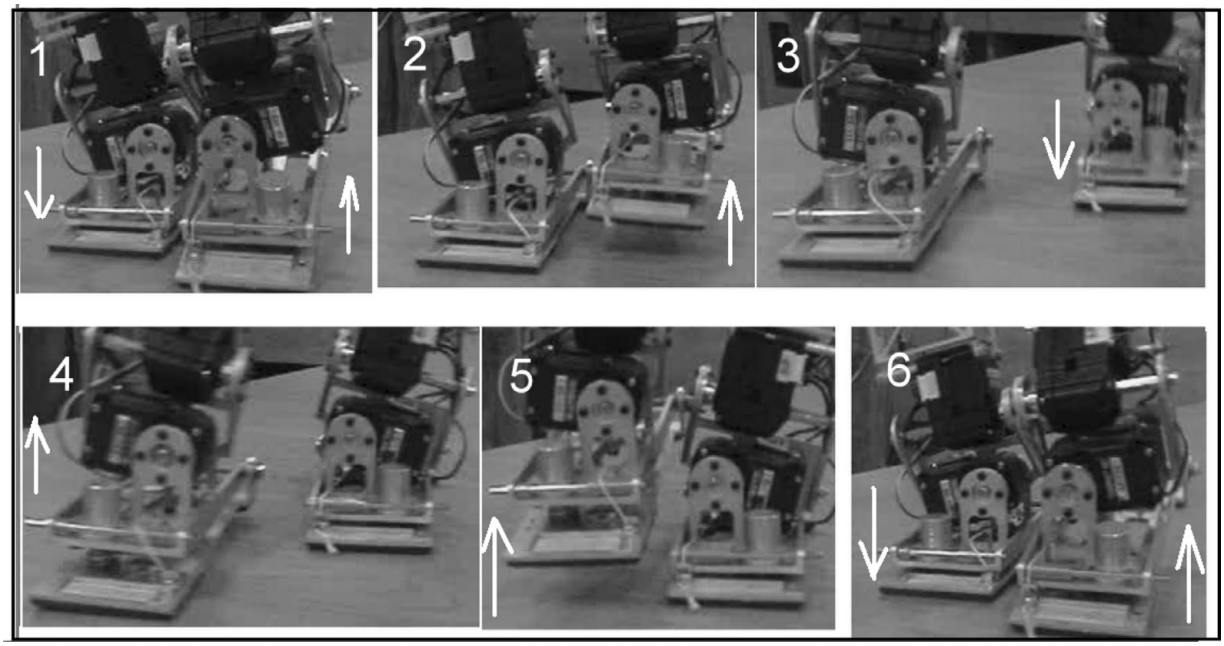

Fig. 20. Back view of the robot feet during the walk: frame 1 – the moment after left leg touched the ground, the spring in right leg is released and leg starts transferring; frame 2 – right leg is in transfer phase and the motor partially compressed its spring, the spring in left leg is fully compressed; frame 3 – right leg just landed, the spring release in left leg will start soon; frame 4 – the full release of the spring in left leg, just before takeoff; frame 5 – left leg in transfer, the foot is still not closed; frame 6 – end of whole cycle (situation as in the frame 1 but after completing one step).

is quite big value, following the robot-human dimensional proportion 1 : 3.7 the range of this displacement should be $(0.06/3.7) = 0.017$. On the other hand, the robot leg masses are not following the human proportions; moreover, the mass of the lower leg is significantly greater than the upper one what is not the human case. Figure 19 shows the sequence of pictures during robot walk. Just recently, we obtained the new results for the walk with spring support. In the beginning of support phase due to the force load, the spring is compressed and then is locked by locker. The spring release starts shortly (240 ms) before leg takeoff; once the leg is in transfer, the motor compresses the spring and closes the foot. The whole walking cycle with one step by each leg lasts 4 s. The spring stiffness is 122 N/m and the active length is 0.024 m. The observed walking performances with active spring are better than those with constantly closed foot, the gait was more robust to the external disturbances. The springs action during the walk is illustrated by sequence of frames selected from recorded movie (see Fig. 20).

4. Conclusions

To obtain the robot movement similar to that of an animal, or totally independent of human decision is still a problem due to the mechanical construction limits, or due to the weaknesses of motion generation methods.

Our target is to use biological inspiration for two-legged robot design and motion controlling. The foot design with spring refers to observed compliance in human gait.[6] For human being this helps in dynamical motion. Only in recent several year, the role of foot in robot locomotion focuses the attention of researchers.[5]

Dynamical simulations and recently performed experiments proved that with our modified robot, it is possible to obtain the stable gait. Such gait saves the energy comparing to the previous prototype.[8] Currently, we started theoretical and experimental study aiming to explain how the springs with different length and stiffness affect the motion properties.

As the final conclusion, it must be noted that the foot compliance obtained by spring is one of the simplest and cheapest solutions. The more advanced designs use flexible actuators with controlled stiffness,[14] they are applied in complex humanoids.

Acknowledgments

The authors gratefully acknowledge the support of this work by the Ministry of Science and Higher Education under Grant No. N514 297935. Robot design and prototyping was done by P. Kryczka – B.Sc. in Engineering. The genetic algorithm method and robot motion modeling for robot with classic feet was done by T. Jargillo – M.Sc. in Engineering. The dynamical simulation and energy efficiency study for the robot with compliant feet was performed by T. Jargillo.

References

1. J. S. Bay and H. Hemami, "Modeling of a neural pattern generator with coupled nonlinear oscillators," *IEEE Trans. Biomed. Eng.* **BME-34**(4), 297–306 (1987).
2. N. A. Bernstein, *The Coordination and Regulation of Movements* (Pergamon, Great Britain, 1967).
3. K. Hirai, M. Hirose, Y. Haikawa and T. Takenaka, "The Development of Honda Humanoid Robot," *Proceedings of the IEEE International Conference on Robotics and Automation (ICRA)*, Leuven, Belgium (May 16–20, 1998) pp. 1321–1326.

https://doi.org/10.1017/S0263574711000300 Published online by Cambridge University Press

4. J. Buchli, L. Righetti and A. J. Ijspeert, "Engineering entrainment and adaptation in limit circle systems. From bilogical inspiration to application in robotics," *Biol. Cybern.* **95**, 645–664 (2006).
5. D. Djoudi and C. Chevallereau, "Feet Can Improve the Stability of a Control Law for Walking Robot," *Proceedings of the IEEE International Conference on Robotics and Automation, Orlando, USA* (May 15–19, 2006) pp. 206–1212.
6. H. Geyer, A. Seyfarth and R. Blickhan, "Compliant Leg Behavior Explains Basic Dynamics of Walking and Running," *Proceedings of the Royal Society*, (2006) doi: 10.1098, published online.
7. A. J. Ijspeert, "Central pattern generators for locomotion control in animals and robots; a review," *Preprint of Neural Netw.* **21**(4), 642–653 (2008).
8. T. Jargillo, The Analysisis of Stiffness Influence on the Gait of Two-Legged Robot – in Polish *M.Sc. Thesis* (Warsaw, Warsaw University of Technology, 2009).
9. K. Matsuoka, "Sustained oscillations generated by mutually inhibiting neurons with adaptation," *Biol. Cybern.* **52**, 367–376 (1995).
10. J. Nakanishi, J. Morimoto, G. Endo, G. Cheng, S. Schaal and M. Kawato, "Learning from demonstration and adaptation of biped locomotion," *Robot. Auton. Syst.* **47**, 79–91 (2004).
11. F. B. Ouezdou, A. Konno, R. Sellaouti, F. Gravez, B. Mohamed and O. Bruneau, "ROBIAN Biped Project – A Tool for the Analysis of the Human-being Locomotion System," *Proceedings of the 5th IEEE International Conference on Climbing and Walking Robots (CLAWAR)* (2002) pp. 212–300.
12. Ch. L. Vaughan, B. L. Davis and J. C. O'Connor, *Dynamics of Human Gait* (Human Kinetics Publishers, 1992).
13. G. M. Thompson, *Introduction to the Study of Human Walking, Kinesiology and Biomechanics* (Department of Biostatistics and Epidemiology, University of Oklahoma Health Sciences Center, 2006).
14. B. Vanderbroght, B. Verrelst, R. Van Ham, M. Van Damme, P. Bey and D. Lefeber, "Development of compliance controller to reduce energy consumption for bipedal robots," *Auton. Robots* **24**, 419–434 (2008).
15. V. M. Ukobratovic and Yu. Stepanenko, "On the stability of anthropomorphic systems," *Math. Biosci.* **15**, 1–37 (1972).
16. M. Vukobratovic and B. Borovac, "Zero-moment point - thirty five years of its life," *Int. J. Humanoid Robot.* **1**(1), 157–173 (2004).
17. D. A. Winter, *Biomechanics and Motor Control of Human Gait: Normal, Elderly and Pathological* (University of Waterloo, 1991).
18. T. Zielinska, "Coupled oscillators utilized as gait rhythm generators of a two-legged walking machine," *Biol. Cybern.* **74**, 263–273 (1996).
19. T. Zielinska, Ch. M. Chew, P. Kryczka and T. Jargilo, "Robot gait synthesis using the scheme of human motion skills development," *Mech. Mach. Theory* **44**(3), 541–558 (2009).